

Electrochemical investigation of anthracen-9-ylmethylene-(3,4-dimethyl-isoxazol-5-yl)-amine compound at gold electrode

A.A. Al-Owais¹, I.S. El-Hallag^{2,*}, E H El-Mossalamy³

¹ Chemistry Department, College of Sciences, King Saud University, Saudi Arabia

² Chemistry Department, Faculty of Science, Tanta University, Tanta, Egypt

³ Chemistry Department, Faculty of Science, Benha University, Benha, Egypt

*E-mail: i.elhallag@yahoo.com

Received: 12 May 2022 / Accepted: 17 June 2022 / Published: 7 August 2022

The electrochemistry investigation of anthracen-9-ylmethylene-(3,4-dimethyl-isoxazol-5-yl)-amine compound at a gold electrode has been achieved via cyclic voltammetry, convolution transforms and numerical simulation techniques at an ordinary Au electrode in 0.1 mol L⁻¹ tetraethylammonium perchlorate (TEAP) in acetonitrile (CH₃CN). The examined substance was oxidized by loss of a single electron producing radical cation tracked by a rapid chemical process and the oxidized form of radical cation convert to a dication via losing of another single electron which followed by a coupled chemical process. The chemical and the electrochemical parameters (α , k_s , E^0 , D , and kc) of the investigated compound were determined via convolutive cyclic voltammetry. The verification of the determined chemical and electrochemical parameters of the investigated compound were executed via numerical simulation method. Based on the above discussion, the electrode pathway was found to proceeds as ECEC mechanism.

Keywords: Anthracen-9-ylmethylene, Electrochemical parameters, Au electrode, Numerical simulation.

1. INTRODUCTION

In organic synthesis isoxazoles are used as five-membered aromatic heterocycles intermediates [1]. The existence of isoxazole moiety may participate to improve the pharmacokinetic profile, lower toxicity, and improve the efficiency [1,2]. The two adjacent electronegative heteroatoms of isoxazole ring are effective for hydrogen donor acceptor interactions [3]. Their lack of cytotoxicity makes them the proper scaffolds for the formation of novel compounds due to their diverse biological activities like: antiparasitic [4], antimicrobial [5-7], antiviral [8,9].

Isoxazole imitative are important compounds which are widely used in the field of therapeutics and pharmaceuticals like insecticidal, antiseptic [10,11], antimycotic, antineoplastic, antibiotic [12,13],

and anticancer [14]. The derivatives of isoxazole are utilized in the market as an emollient to relieve inflammation sedatives [15]. Isoxazole derivatives have been used in commercial utilization for numerous years [16-18]. Acivicin is an antileishmania, anti-carcinoma sedative, while isoxaflutole is used as herbicidal sedative [19,20]. The associations of different substructures are the one of the approaches to synthesize probable organic active compounds from known operative compositions.

To the best of our information, there are no electrode pathway examinations of Anthracen-9-ylmethylene-(3,4-dimethyl-isoxazol-5-yl)-amine carried out on Au surface cathode in CH₃CN and TEAP as indifferent electrolyte. So, in this work we examined the voltammetric consideration of Anthracen-9-ylmet-hylene-(3,4-dimethyl-isoxazol-5-yl)-amine via convolutive cyclic voltammetry & numerical model. The chemical and electrochemical factors were calculated experientially and established via the method of numerical representation.

2. EXPERIMENTAL

2.1. Chemicals.

The anthracen-9-ylmethylene-(3,4-dimethyl-isoxazol-5-yl)-amine compound in a state of exam-ination was synthesize according to the method established in literature as following [21]:

5-amino-3,4-dimethylisoxazole (0.0024 mol) and anthracene-9-carbal-dehyde (500 mg, 2.4 mM) in ethyl alcohol (15 mL) was heated for 120 min. TLC was utilized for observation the advancement of the reaction. The isolated solid from the chilly concoction was accumulated and recrystallized from the chloroform – methyl alcohol mixture (2: 8) to produce the heading compound. Yellow solid: Yield: 82%;m.p. 146-147 °C.

GC-MS m/z (rel. int.%): 301 (62) [M+1]⁺.

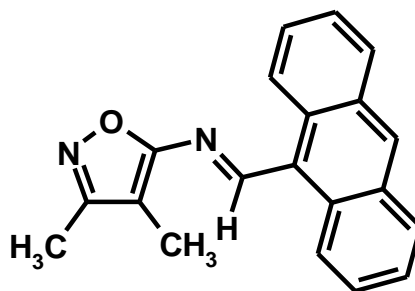
IR (KBr) ν_{\max} cm⁻¹: 2917 (C-H), 1580 (HC=N), 1158 (C-N).

¹H NMR (600MHZ, CDCl₃) (δ /ppm): 10.12 (s, CH olefinic), 8.95 (d, 2H, H1, J = 8.8 Hz), 7.61 (dd, 2xH, H2, J=5.6 Hz), 7.50 (dd, 2xH, H3, J=7.2 Hz), 8.56 (d, 2H, H4 J=8.0 Hz), 7.65 (s, H5), 2.30 (s, CH₃), 2.16 (s, CH₃).

¹³CNMR (600 MHz, CDCl₃) δ : 165.44, 162.07, 159.82, 132.63, 131.53, 131.10, 130.05, 129.27, 129.12, 127.94, 125.54, 124.07, 123.56, 116.50, 108.03, 10.83, 6.89.

Anal. calc. for C₂₀H₁₆N₂O: C, 79.98, H, 5.37, N, 9.33. Found: C, 79.94, H, 5.32, N, 9.28

Scheme 1 shows the structure of the isoxazole derivative under investigation.



Scheme 1

2.2. Voltammetric examinations.

Convulsive transforms and voltammetric study were executed employing a Princeton Applied Research (PAR) Computer – controlled Potentiostat Model 283 and PAR Model 175 Universal Program (from EG and G). The apparatus accepted the handling of scan rate until 100 V/s for the cyclic voltammetric examination.

Three ordinary electrode cell configurations were utilized for electrochemical analyses. The working electrode was Au with surface area $7.85 \times 10^{-3} \text{ cm}^2$, coiled Pt wire as a CE and the RE was soaked Ag/AgCl.

The voltage of the active electrode was considered with a comparative to the potential of Ag/AgCl reference electrode at 25°C and 0.1 mol/L tetraethylammonium perchlorate (TEAP) as indifferent electrolytic capacitor. Solution impedance and double layer condenser current of the cyclic voltammetry data were reduced by background subtraction of condenser current and iR adjustments compensation. The cleaning of the active electrode was done on a polisher Ecomet hoagy. Data of cyclic voltammetry studies were recorded at scan rate in the range of 0.02 to $2\text{V}\cdot\text{s}^{-1}$ in non-aqueous media at $(25 \pm 2)^\circ\text{C}$.

The Numerical model of the experimental cyclic voltammograms was performed on PC computer utilizing condesim program purchased from EG & G. Algorithms used in the numerical program were coded and implemented in the condesim software program supplied by EG & G.

Oxygen free nitrogen was run into the cell contents for 15 minutes and a N_2 gas was kept up the solution during the whole of the experiments to expel the air from the working solutions under investigation.

3. RESULTS AND DISCUSSION

3.1. Voltammetric studies

The recorded points of i-E plot of $3 \times 10^{-4} \text{ M}$ of the examined anthracen-9-ylmethylene-(3,4-dimethyl-isoxazol-5-yl)-amine compound in CH_3CN solvent, at scan rate of $0.001 \text{ V}\cdot\text{s}^{-1}$ is manifested in Figure 1. As noted in Figure 1, at low scan rate, the first oxidation peak not associated with a reduction peak in the opposite direction, and the second oxidative peak not combined with a cathodic peak in the reversal sweep too. This character confirms that the rate of homogeneous rate constant (k_c)

of the chemical process is too fast at low scan rate. The cyclic voltammograms at different values of scan rates are summarized in Figure 2.

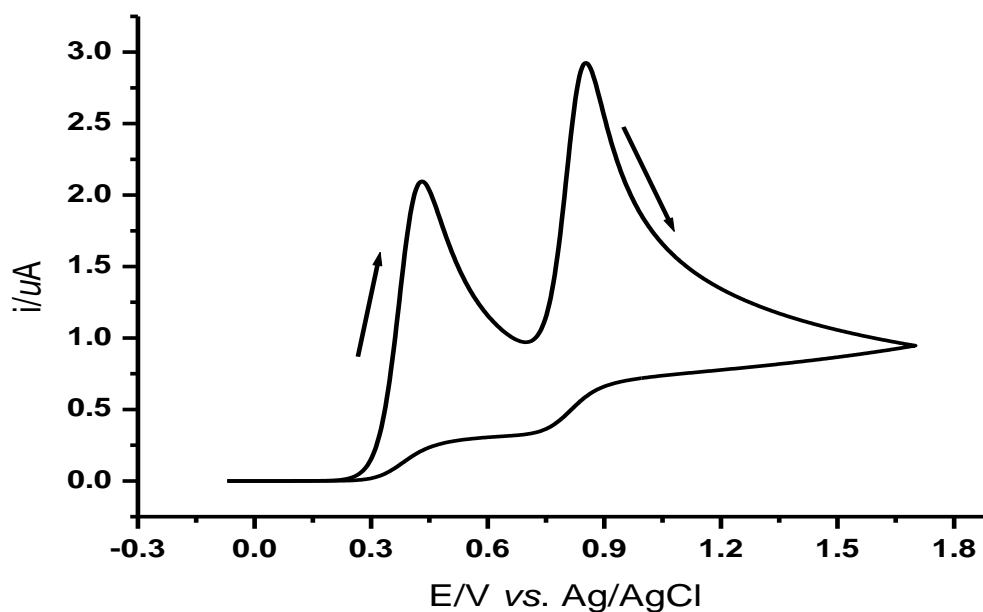


Figure 1. Cyclic voltammogram of 3.0×10^{-4} M of isoxazole at a gold electrode in $\text{CH}_3\text{CN}/0.1\text{M TEAP}$, at scan rate of $0.001 \text{ V} \cdot \text{s}^{-1}$ and $25 \text{ }^\circ\text{C}$

3.1.1. Influence of scan rate

In this manuscript the electrode reaction of the examined isoxazole imitative exhibited an increasing of peak current with increasing of the scan rate, and the location of the onward peak potentials of the oxidative anodic process were displaced to more positive values of voltages. From the recorded cyclic voltammograms, it was concluded that, the rate of electron transfer of oxidative step of the isoxazole is sluggish at all scan rates. The nonappearance of the reduction peaks in the reversal path at low values of the scan rate proves the presence of rapid chemical step preceded by the electron transfer. This situation revealed that the first electron transfer results in a cation radical followed by a rapid chemical reaction and the radical cation produces another one electron to produce a dication which followed by a rapid chemical process. Investigation of Figure 2 shows that, at high scan rate, the first oxidation peak (A_1) was associated with a small reduction peak (C_1) in the opposite scan, while the second oxidative peak (A_2) was associated with a small cathodic peak (C_2) in the opposite scan. The ratio of the reversal peak to the forward peak (i_{pb}/i_{pf}) is less than unity for the two oxidation peaks, confirming that the rapidity of the rate of the homogeneous rate constant (k_c) of the chemical

process. The oxidation peak currents, subsequent to the minimization of the residual current, is proportional to the square root of scan rate ($v^{1/2}$).

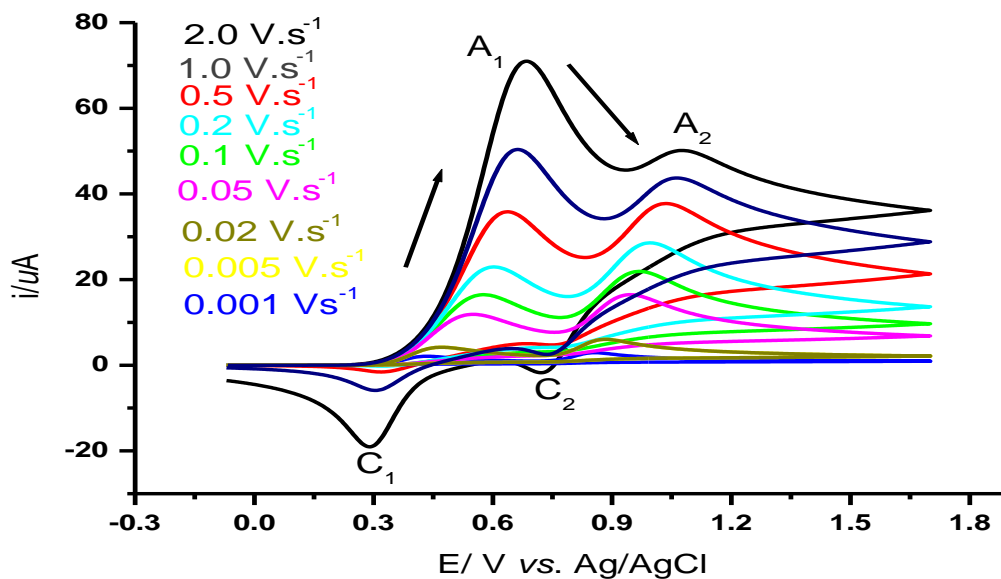


Figure 2. Cyclic voltammograms of 3×10^{-4} M of the anthracen-9-ylmethylene-(3,4-dimethyl-isoxazol-5-yl)-amine at a Au electrode in $\text{CH}_3\text{CN} / 0.1\text{M TEAP}$, at various scan rates and $T 25^\circ\text{C}$.

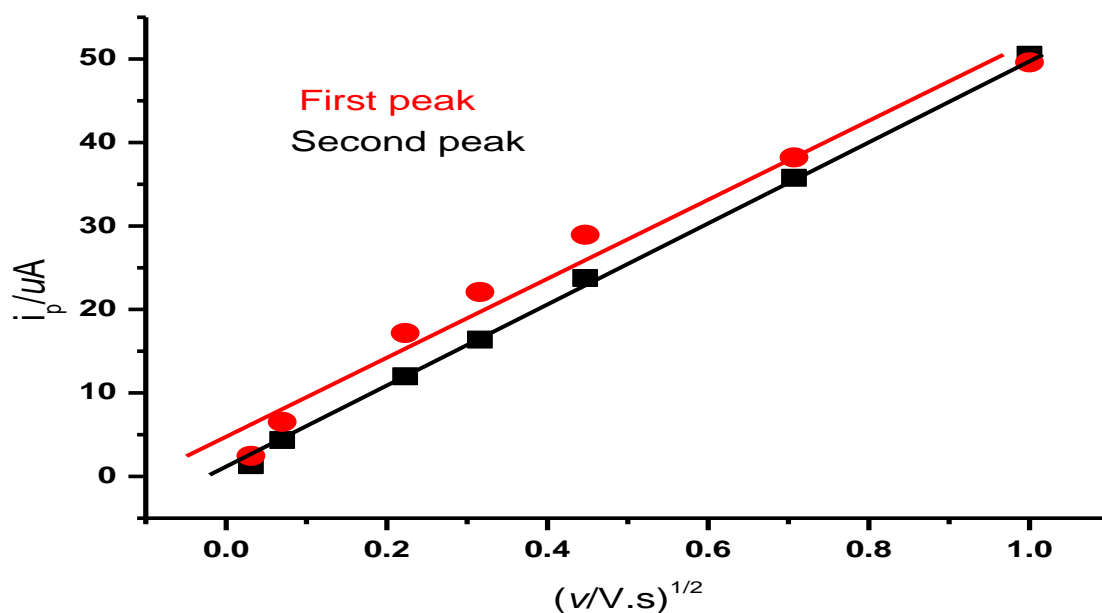


Figure 3. The plot of i_p vs \sqrt{v} of oxidation process of the 3×10^{-4} M anthracen-9-ylmethylene-(3,4-dimethyl-isoxazol-5-yl)-amine at a Au electrode and $T 25^\circ\text{C}$.

The sluggishness character of the electron transfer in 0.1 mol/L TEAP/CH₃CN was ascertained from the values of peak potential distance ΔE_p . The values of ΔE_p were in the extent of 360 – 520 & 400 – 623 mV of the first and the second electron transfers sequentially, the value of the mean local position of the onward and reversal peak potentials produces the magnitude of the redox potential (E^0) (table 1).

The value of rate constant of heterogeneous electron transfer (k_s) was derived from the functioning curve listed in literature [22]. The diffusion factor (D) of the derivative of the isoxazole under examination was calculated from the plot of i_p vs. \sqrt{v} [22,23]. Accordingly, the calculated values of k_s and D were cited in Table 1. As shown in Fig. 3, the plot of i_p vs \sqrt{v} display straight line for the two oxidation peaks of examined isoxazole confirming the electrode nature proceeds mainly by diffusion process [23].

3.1.2. Presentation of i_p versus E_p

As noted, enhancing v generally increases the current and causes the position of peak potential to shift to more positives values.in the direction of the scan.

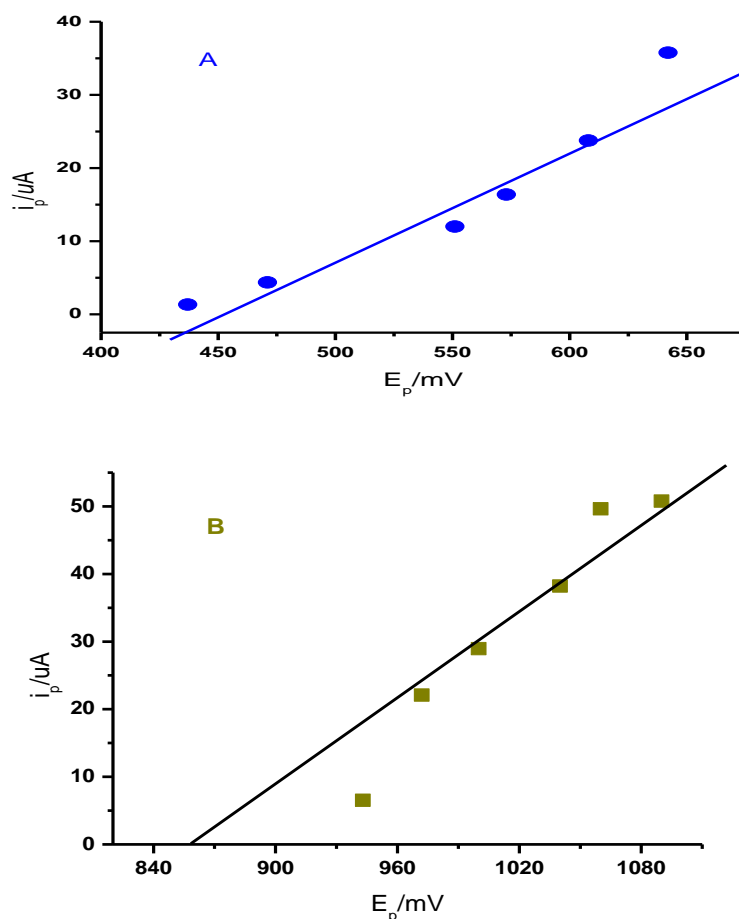


Figure 4. Plots of i_p vs. E_p by CV of the first (A) and the second (B) peak of 3×10^{-4} M of the anthracen-9-ylmethylene-(3,4-dimethyl-isoxazol-5-yl)-amine at a Au electrode in CH₃CN/0.1M TEAP, at various scan rates and T 25 °C.

Although i_p is related strongly with E_p , the relationship has rarely been examined quantitatively. A technique of analyzing the potential shift is to plot i_p against E_p , [24] as shown in Figure 4. The potential extrapolation to the zero current on each straight line should be close to the redox potential (E^0). As shown in Figure 4 the values of intercept for the first and second peaks are 0.432 V and 0.863 V respectively which very close to the values of redox potential cited in table 1.

3.1.3. $i-t$ curve derived from cyclic voltammogram

The $i-t$ plot extracted from CV of the oxidation approaches of the compound under examination at sweep rate of $0.001 \text{ V}\cdot\text{s}^{-1}$ is manifested in Fig.5 [25]. By way of taking the data points of the decayed part of the $i-t$ plot and presentation it as current (i) versus $1/(t)^{1/2}$ which produce a Cottrell plot. The slope of Cottrell plots of the isoxazole species allows a diffusion coefficient cited in Tables 1. As demonstrated in Fig.5 the $i-t$ plots produce discontinuation Δi_c at $t = 17.00 \text{ s}$ due to the convertibility of the scan. Analysis of Fig.5 exhibited that, the lack of equality of the highness of the moving forward and reversed directions, i.e. the height of the forward peak is more than that of the backward peak confirming the presence of a chemical step beyond electron transfer process.

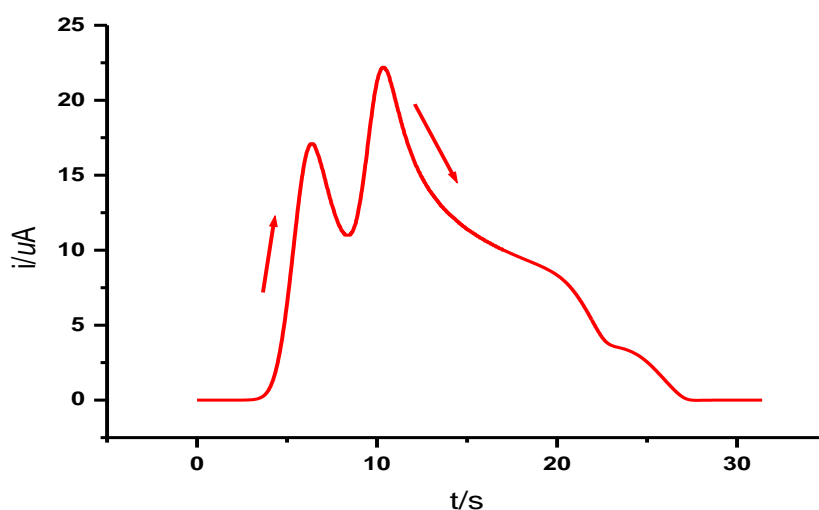


Figure 5. Plot of i vs. t of $3 \times 10^{-4} \text{ M}$ oxidation process of the anthracen-9-ylmethylene-(3,4-dimethylisoxazol-5-yl)-amine at Au electrode, scan rate of $0.001 \text{ V}\cdot\text{s}^{-1}$ and $T 25 \text{ }^\circ\text{C}$.

Figure 6 provides the experimental and numerical curves of the isoxazole compound, which validate good agreement between the theoretical $i-E$ plot and the captured one with some anomaly of the second wave which could be coming from some sort of iR drop due to the resistance of the cell solution.

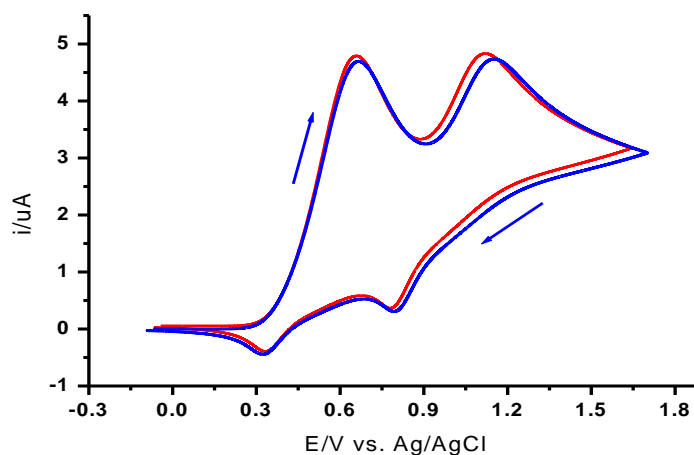


Figure 6. Compare between experimental voltammogram of the anthracen-9-ylmethylene-(3,4-dimethyl-isoxazol-5-yl)-amine (red) and simulated voltammogram (blue) at a sweep rate of $1.0V \cdot s^{-1}$ and $T 25 \text{ }^\circ C$

3.1.4. Convolutional transforms.

It was established that, the convolution theorem gives [26-29]:

$$L^{-1}[f_s(S) \cdot g_s(S)] = \int_0^t G(u)F(t-u)du \tag{1}$$

in which f_s & g_s are the Laplace transforms of the functions F and G , and the symbol u is a dummy variable which is lost when the definite integral is calculated. In the following reaction:



in which the initial species loss only simple electron transfer and no subsequent processes exist with the 'linear' diffusion from a planar electrode, i.e., the Fick's second law is written as [29]:

$$\left[\frac{\partial C_A}{\partial t} \right]_x = D_A \left[\frac{\partial^2 C_A}{\partial x^2} \right]_x \tag{2}$$

the I_1 convolution is expressed by $I_1 = i^*(\pi t)^{-1/2}$ or more 'fully' in the form:

$$I_1(t) = \pi^{-1/2} \int_0^t i(u)/(t-u)^{1/2} du \quad (3)$$

Various algorithms have been suggested for the assessment of the convolution $I(t)$. Here, the coming one was utilized [28-37]:

$$I_{(t)} = I(k\Delta t) = \frac{1}{\sqrt{\pi}} \sum_{j=1}^{j=k} \frac{\Gamma\left(k-j+\frac{1}{2}\right)}{(k-j)!} \cdot \Delta t^{\frac{1}{2}} i(j\Delta t) \quad (4)$$

where $I(j\Delta t)$ is the current taken at equally interspaced time intervals Δt and $\Gamma(x)$ is the Gamma function of x .

The D value for the oxidation processes were determined using equation (5):

$$I_{lim} = nFAC\sqrt{D} \quad (5)$$

and registered in Table 1. Figure 7 displays the I_1 convolution of the oxidation wave at $1.0 \text{ V}\cdot\text{s}^{-1}$ scan rate. The large space between the reversal scan and the forward one of the I_1 convolution demonstrate the sluggishness character of electron transfer. Also, the reversal direction does not reach to zero value of current, confirming the existence of chemical process combined with electron exchange and the stagnant kinetic nature of the heterogeneous rate constant (k_s) between the electroactive isoxazole compound and the electrode surface, *i.e.*, the mechanistic pathway behaves as *ECEC*.

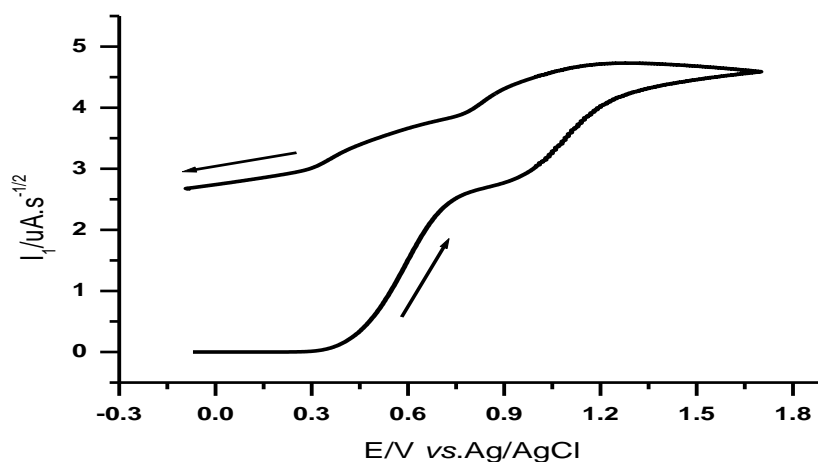


Figure 7. Convolution voltammetry (I_1) of the anthracen-9-ylmethylene-(3,4-dimethyl-isoxazol-5-yl)-amine at Au electrode, scan rate of $1.0 \text{ V}\cdot\text{s}^{-1}$, T 25°C .

The established convoluted current (I_{limd}) was used for evaluation of D value from the relationship (6) [25,28]:

$$I_{limd} = \frac{i_p}{3.099(\alpha n a \nu)^{1/2}} \quad (6)$$

where I_{limd} is the limiting of deduced convolution current ($I_{limd}=I_{lim} = nFAC\sqrt{D}$). It was found that the values of D calculated from the cyclic voltammetry and equation (5) agree well with the values calculated from equation (6) (table 1). The rate constant (k_c) of homogeneous chemical reaction of the first step was established via I_2 convolution, as shown in figure 8 which consider simple, fast, precise, and accurate method [23]. The estimated values of k_c were recorded in Table 1. The true homogeneous chemical rate constant (k_c) of the chemical step was evaluated precisely via the kinetic convolution (I_2) at a sweep rate of $1.0 \text{ V}\cdot\text{s}^{-1}$, by introducing the test values of the homogeneous chemical rate constant (k_c) into the I_2 convolution until I_2 reached to zero immediately after the peak as shown in figure 8 [23]. The true k_c value determined from I_2 convolution of the first oxidation wave was found to be 2.21 s^{-1} which agrees well with the value used in numerical cyclic voltammograms.

Table 1. Electrochemical parameters of the anodic oxidation processes of isoxazole derivative compound

E^{o1} ,	E^{o2} ,	$k_{s1}\times 10^3$	$k_{s2}\times 10^3$	$D1\times 10^9$	$D2\times 10^9$	α_1	α_2	k_{c1}	k_{c2}
V	V	$\text{cm}\cdot\text{s}^{-1}$	$\text{cm}\cdot\text{s}^{-1}$	$\text{cm}\cdot\text{s}^{-1}$	$\text{cm}\cdot\text{s}^{-1}$			s^{-1}	s^{-1}
0.430 ^a	0.852	2.20	2.50	5.20	5.20	0.33	0.36	---	---
0.434 ^b	0.853	2.12	2.80	5.81	5.90	0.33	0.35	2.2	2.7
---	---	---	---	5.58	5.70	---	---	---	---
0.440 ^d	0.853	---	---	5.42	5.22	---	---	2.21 ^f	---
---	---	---	---	5.51 ^e	5.13 ^e	---	---	---	---
0.410 ^g	0.802	2.00	2.40	6.21	6.53	0.48	0.39	0.40	0.30

Values determined from (a) experimental work (b) numerical simulation, (c) via Eq. (5), (d) via Eq. (6), (e) via Eq. (10), (f) from the kinetic convolution, and (g) reference [38].

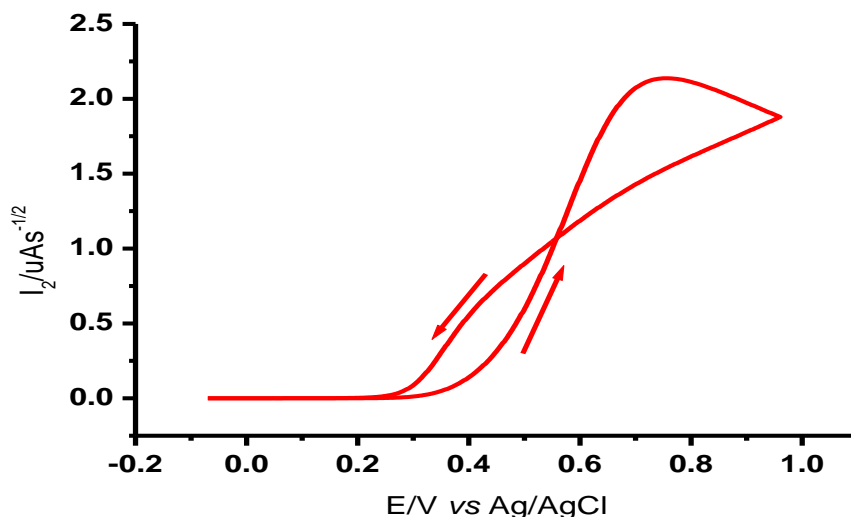
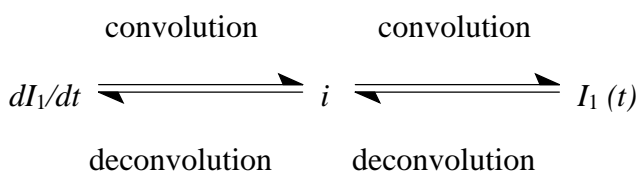


Figure 8. Kinetic convolution current of the first oxidation peak of the examined anthracen-9-ylmethylene-(3,4-dimethyl-isoxazol-5-yl)-amine at a Au electrode, scan rate 1 V·s⁻¹ and T 25 °C.

3.3. Deconvolution transforms.

The relationship between $t^{-1/2}$ convolutions and deconvolutions is indicated as following [38]



The deconvoluted transforms (dI_1 /dt) as a function of E of the fast kinetic process is described as [38-42]:

$$\frac{dI_1}{dt} = \frac{nFAC\sqrt{D}\alpha\zeta}{(1+\zeta)^2} \tag{7}$$

where $\alpha = \frac{nvF}{RT}$ (8)

and $\zeta = \exp[nF/RT(E - E^0)$ (9)

and the deconvoluted transforms at $v = 0.6 \text{ V}\cdot\text{s}^{-1}$ are summarized in Fig. 9. The wave width of deconvoluted transforms (w_p) in the case of fast kinetics is equal to $3.53 RT/nF = 90.5 /n \text{ mV}$. It was found that $w_p = 250 \pm 5 \text{ mV}$ and $0.224 \pm 5 \text{ mV}$ for first and second wave respectively, demonstrating and ascertain the sluggishness kinetic nature of electron transfer of the electrode pathway at high sweep rate.

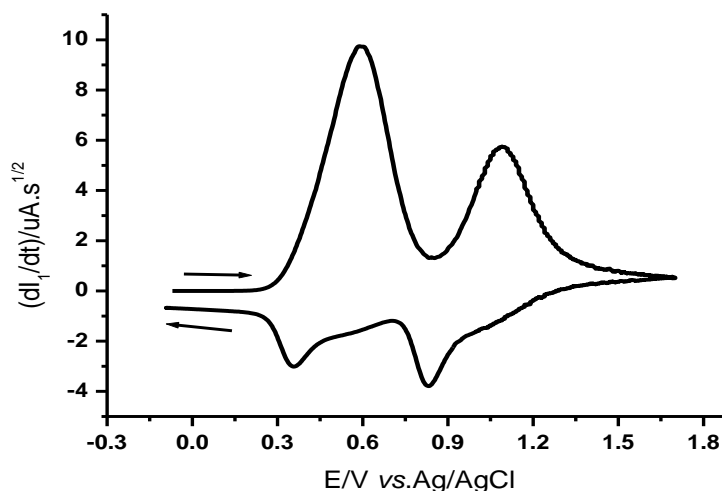


Figure 9. Deconvolution voltammetry (dI_1/dt) of anthracen-9-ylmethylene-(3,4-dimethyl-isoxazol-5-yl)-amine at a Au electrode, a sweep rate $1 \text{ V}\cdot\text{s}^{-1}$ and $T 25^\circ\text{C}$.

The separation and the non-symmetry of the forward and reverse sweep, further validating the stagnant kinetic nature of electron transfer for ECEC pathway of the oxidation processes of isoxazole derivative. The standard redox potentials were determined from the average values of deconvoluted peak potentials of the two peaks (table 1). It was noted that the values of E^0_1 & E^0_2 evaluated from deconvoluted transforms agree well with the values calculated from the cyclic voltammograms and numerical simulation (table 1).

It was found that the extent of the peak of (dI_1/dt) transform is correlated to the total concentration of the investigated isoxazole compound, the surface area of the electrode, and the scan rate ν . As illustrated in Fig.9 the peak width of the second wave is narrower than the first one proving that the second electron transfer is faster than the first one. The value of D was also evaluated using Eq. (10) [26-30]

$$ep = \frac{\alpha n^2 F^2 \nu C^{bulk} D^{1/2}}{3.367 RT} \quad (10)$$

where e_p is the wave extent (in ampere) of the onward sweep and the remaining terms have their normal meanings. The Values of D derived using equation (10) are indicated in Table 1.

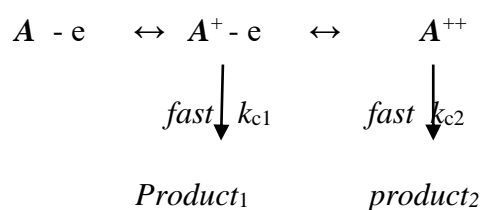
Also, from combination between the convolution and deconvolution voltammetry, Eq. (11) was deduced

$$n = \frac{ep3.367RT}{\alpha F \nu I_{lim}}$$

$$n = \frac{0.086ep}{I_{lim}\alpha v} \quad (11)$$

where n is the number of electrons involved in the electrode pathway, and the other symbols have their normal definitions. From Eq. (11) the total number of electrons consumed in the electrode reaction was calculated and found to be 2.01. The simple method for estimation of the total number of electrons involved in the electrode reaction using Eq. 11 without knowing the electrode surface area can be considered an accurate method for the determination of the number of electrons.

Based on the above electrochemical discussion, the electrode mechanistic pathway of anthracen-9-ylmethylene-(3,4-dimethyl-isoxazol-5-yl)-amine can be suggested to proceed as:



i.e., *ECEC* mechanism.

4. CONCLUSION

The electrochemical examination of isoxazole imitative in 0.1 M TEAP /CH₃CN at a Au electrode revealed that the presence of two oxidation peaks (A₁ & A₂) associated with two small reduction peaks (C₁ & C₂). This attitude indicates that the first charge exchange produces a radical cation in the first step and the second step loss another electron to form dication. The experimental kinetic parameters were evaluated experimentally and ascertained via numerical method by comparing the generated numerical voltammograms against the experimental voltammograms. The passageway of electrode mechanism was proposed to proceed as *ECEC* system.

ACKNOWLEDGEMENT

This project was supported by King Saud University, Deanship of Scientific Research, College of Science Research Center.

References

1. F. Hu and M. Szostak, *Adv. Synth. Catal.*, 357 (2015) 2583.
2. J. Zhu, J. Mo, H. Lin, Y. Chen, and H. Sun, *Biorg. Med. Chem.* 26 (2018) 3065.
3. G. N. Pairas, F. Perperopoulou, P.G. Tsoungas and G. Varvounis, *ChemMedChem* 12 (2017) 408.
4. A. De Souza, V. Xavier, G. Coelho, P. Sales Junior, A. Romanha, S. Murta, C. Carneiro and J. Taylor, *J. Braz. Chem. Soc.* 29 (2017) 269.

5. E.A. Musad, R. Mohamed, B.A. Saeed, B.S. Vishwanath and K.L. Rai, *Bioorg. Med. Chem. Lett* 21 (2011) 3536.
6. A. Padmaja, T. Payani, G.D. Reddy and V. Padmavathi, *Eur. J. Med. Chem.* 44 (2009) 4557.
7. A.R. Banpurkar, S.S. Wazalwar and F. Perdih, *Bull. Chem. Soc. Ethiop.* 32 (2018) 249.
8. F. Li, Y. Hu, Y. Wang, C. Ma and J. Wang, *J. Med. Chem.* 60 (2017) 1580.
9. M. Schmidtke, P. Wutzler, R. Zieger, O.B. Riabova and V.A. Makarov, *Antivir. Res.* 81 (2009) 56.
10. P. Cali, L. Naerum, S. Mukhija and A. Hjelmencrantz, *Bioorg. Med. Chem. Letters.*, 14 (2004) 5997.
11. M. Sree Rama Murthy, D. Venkata Rao, and E. Venkata Rao, *Indian J. Pharma. Sci.*, 45 (1983) 131.
12. B. E. Kumara Swamy, *Der Pharma Chemica*, 3 (2011) 224.
13. D. D. Guy and P. M. Carabates, (Sterling Drug Inc.) U.S. 4, 268, 678 (C1. 548-247; C07D261/ 08), 19 May (1981), Appl. 72,134, 04 Sep (1979); 4 pp; *Chem. Abstr.*, 1981, 95, 203923n.
14. G. Daidone, D. Raffa, B. Maggio, F. Plescia, V. M. C Cutuli, N.G. Mangano, and A. Caruso, *Arch. Pharm. Pharm. Med. Chem.*, 50 (1999) 332.
15. S. Balalaie, A. Sharifi and B. Ahangarian, *Indian J. Heterocyclic Chem.*, 10, (2000) 149.
16. L. D. Nunno, P. Vitale, A. Scilimati, S. Tacconelli, and P. Patrignani, *J. Med. Chem.*, 47 (2004) 4881.
17. V. H. Bhaskar and P. B. Mohite, *J. Optoelectron Adv. Mat.*, 2 (2010) 249.
18. M. Sechi, L. Sannia, F. Carta, M. Palomba, R. Dallochio, A. Dessi, M. Derudas, Z. Zawahir and N. Neamati, *Antiviral Chem. Chemother.*, 16 (2005) 41.
19. B. Frolund, A. T. Jorgensen, L. Tagmose, T. B. Stensbol and H. T. Vestergaard, C. Engblom, U. Kristiansen, C. Sanchez, P. Krogsgaard-Larsen, T. Liljefors, *J. Med. Chem.*, 45 (2002) 2454 .
20. B. L. Deng, M. D. Cullen, Z. Zhou, T.L. Hartman, R. W. Buckheit(jr.), C. Pannecouque, E. Declesq, P.E. Fanwick and M. Cushman, *Bioorg. Med. Chem.*, 14, (2006) 2366.
21. A.M. Asiri and S. A. Khan, *Molbank* 2011 (3) M736
22. R.S. Nicholson and I. Shain, *Anal. Chem.*, 37 (1965) 1351
23. S.A. El-Daly, I.S. El-Hallag, E.M. Ebeid, M.M and Ghoneim., *Chin. J. Chem*, 27, (2009) 241.
24. C. Zhang, K.J. Aoki, J. Chen, T. Nishiumi, *J. Electroanal. Chem.*, 708 (2013) 101.
25. A. R. Barron, C. W. Duncan, Jr. - Welch, *Physical Methods in chemistry and nano science*, Connexions, Rice University, 2021.
26. W. J. Bowden, *J. Electrochem. Soc.*, 129 (1982) 124
27. E.H. Wong, and R.M. Kabbani, *Inorg. Chem.*, 19 (1980) 451.
28. I.S. El-Hallag, M.M. Ghoneim and E. Hammam, *Anal. Chim. Acta*, 414 (2000) 173.
29. A. J. Bard and L.R. Faulkner, *Electrochemical Methods, Fundamentals and Applications*, Wiley, New York, 1980.
30. I.S. El-Hallag and A.M. Hassanien. *Collect. Czech. Chem. Commun.*, 64, (1999) 1953.
31. I.S. El-Hallag and M.M. Ghoneim, *Monatsh. Chem.*, 130 (1999) 525.
32. A.R. Seidle and L. Todd. *J. Inorg. Chem.*, 15 (1976) 2839.
33. R. Hettrich, M. Kaschke, H. Wadepohl, W. Weinmann, M. Stephan, H. Pritz-kow, W. Siebert, I. Hyla-Kryspin and R. Gleiter. *Chem. Eur. J.*, 2 (1996) 487.
34. A.A. Al-owais and I. S. El-Hallag, *Int. J. Electrochem. Sci.*, 16 (2021) 210637
35. A.A. Al-owais, I. S. El-Hallag, and E. H. El. Mossalamy, *Int. J. Electrochem. Sci.*, 17 (2022) 22063
36. G. Doetsch, *Laplace Transformation*, Dover, New York, 1953.
37. K.B. Oldham and R.A. Osteryoung, *J. Electroanal. Chem.*, 11 (1966) 397.
38. A.A. Al-Owais and I.S. El-Hallag, *J. New. Mat. Electrochem. Systems*, 18, (2015) 177.
39. J. Galvez and Su.M. Park. *J. Electroanal. Chem.*, 235 (1987) 71.
40. I.S. El-Hallag, Ph.D. Thesis, Tanta University, Egypt (1991).

41. H.M. Al-bishri, I.S. El-Hallag and E.H. El-Mossalamy. *J. New. Mat. Electrochem. Systems*, 14 (2011) 51.
42. A.M. Asiri, S.A. Khan and I.S. El-Hallag. *J. New. Mat. Electrochem. Systems*, 14 (2011) 251.
43. I.S. El-Hallag and S.A. El-Daly, *Bull. Korean Chem. Soc.*, 31 (2010) 989.

© 2022 The Authors. Published by ESG (www.electrochemsci.org). This article is an open access article distributed under the terms and conditions of the Creative Commons Attribution license (<http://creativecommons.org/licenses/by/4.0/>).